Journal of Saudi Chemical Society (2010) **14**, 399–407

King Saud University

Journal of Saudi Chemical Society

www.ksu.edu.sa
www.sciencedirect.com

ORIGINAL ARTICLE

Molecular modeling of 3,4-pyridinedicarbonitrile dye sensitizer for solar cells using quantum chemical calculations

M. Geetha [a], P. Senthil Kumar [a], K. Vasudevan [a], A. Prakasam [a], G. Meenakshi [b], P.M. Anbarasan [a,*]

[a] *Department of Physics, Periyar University, Salem 636 011, Tamil Nadu, India*
[b] *Department of Physics, K.M.C.P.G.S, Lawspet, Puducherry 605 008, India*

Received 1 April 2010; accepted 10 May 2010
Available online 31 May 2010

KEYWORDS

Dye sensitizer;
Density functional theory;
Vibrational spectra;
Electronic structure;
Absorption spectrum

Abstract The geometries, electronic structures, polarizabilities, and hyperpolarizabilities of organic dye sensitizer 3,4-pyridinedicarbonitrile was studied based on Hartree–Fock (HF) and density functional theory (DFT) using the hybrid functional B3LYP. Ultraviolet–visible (UV–Vis) spectrum was investigated by time dependent DFT (TD-DFT). Features of the electronic absorption spectrum in the visible and near-UV regions were assigned based on TD-DFT calculations. The absorption bands are assigned to $\pi \rightarrow \pi^*$ transitions. Calculated results suggest that the three lowest energy excited states are due to photoinduced electron transfer processes. The interfacial electron transfer between semiconductor TiO_2 electrode and 3,4-pyridinedicarbonitrile is due to electron injection process from excited dye to the semiconductor's conduction band. The role of cyanine in 3,4-pyridinedicarbonitrile in geometries, electronic structures, and spectral properties were analyzed.

1. Introduction

The new technologies for direct solar energy conversion have gained more attention in the last few years. In particular, dye sensitized solar cells (DSSCs) are promising in terms of efficiency and low cost (Regan and Gratzel, 1991; Gratzel, 2001; Park and Kim, 2008). The primary feature of DSSC consists in a wide band gap nanocrystalline film grafted with a quasi-monolayer of dye molecules and submerged in a redox electrolyte. This elegant architecture can synchronously address two critical issues of employing organic materials for

* Corresponding author. Tel.: +91 0427 2345766/2345520; fax: +91 0427 2345565/2345124.
E-mail address: anbarasanpm@gmail.com (P.M. Anbarasan).

1319-6103 © 2010 King Saud University.
Open access under CC BY-NC-ND license.
doi:10.1016/j.jscs.2010.05.002

Production and hosting by Elsevier

the photovoltaic applications: (i) efficient charge generation from the Frenkel excitons and (ii) long-lived electron–hole separation up to the millisecond time domain. The latter attribute can often confer an almost quantitative charge collection for several micrometer-thick active layers, even if the electron mobilities in nanostructured semiconducting films are significantly lower than those in the bulk crystalline materials. Benefited from systematic device engineering and continuous material innovation, a state of the art DSSC with a ruthenium sensitizer has achieved a validated efficiency of 11.1% (Chiba et al., 2006) measured under the air mass 1.5 global (AM1.5G) conditions. In view of the limited ruthenium resource and the heavy-metal toxicity, metal-free organic dyes have received surging research interest in recent years (Hara et al., 2003; Kitamura et al., 2004; Horiuchi et al., 2004; Campbell et al., 2004; Thomas et al., 2005; Hagberg et al., 2006; Li et al., 2006; Koumura et al., 2006; Kim et al., 2006; Wang et al., 2007, 2008; Edvinsson et al., 2007; Shi et al., 2008; Zhou et al., 2008; Lin et al., 2009; Zhang et al., 2009; Xu et al., 2009). The ruthenium dye and the flexibility in molecular tailoring of an organic sensitizer provides a large area to explore for the reason that of their high molar absorption coefficient, relatively simple synthesis procedure, various structures and lower cost (Zhang et al., 2007; Liang et al., 2007; Xu et al., 2008). Moreover, recently a rapid progress of organic dyes has been witnessed reaching close to 10.0% efficiencies in combination with a volatile acetonitrile-based electrolyte (Ito et al., 2008). In this paper the performance of 3,4-pyridinedicarbonitrile metal-free dye that can be used in DSSC is analyzed.

2. Experimental details

The compound 3,4-pyridinedicarbonitrile was obtained from Sigma–Aldrich Chemical Company, USA with a stated purity of greater than 99% and it was used as such without further purification. The FT-Raman spectrum of 3,4-pyridinedicarbonitrile has been recorded using 1064 nm line of Nd:YAG laser as excitation wavelength in the region 50–3500 cm^{-1} on a Brucker model IFS 66 V spectrophotometer. The FT-IR spectrum of this compound was recorded in the region 400–4000 cm^{-1} on IFS 66 V spectrophotometer using KBr pellet technique. The spectrum was recorded at room temperature, with scanning speed of 30 cm^{-1} min^{-1} and the spectral resolution of 2.0 cm^{-1}.

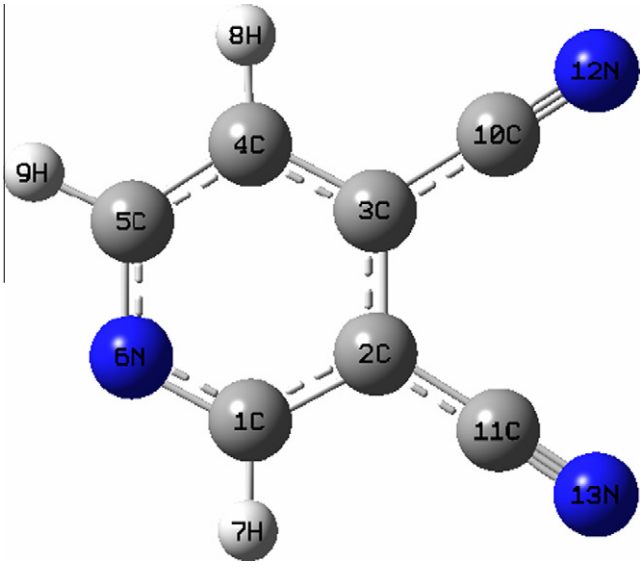

Figure 1 Optimized geometrical structure of dye 3,4-pyridinedicarbonitrile by B3LYP/6-311++G(d,p).

Table 1 Bond lengths (Å), bond angles (°) and dihedral angles (°) of the dye 3,4-pyridinedicarbonitrile.

Parameters	HF/6-311++G(d,p)	B3LYP/6-311++G(d,p)
Bond length (Å)		
C1–C2	1.3893	1.4034
C1–N6	1.3147	1.3292
C1–H7	1.0749	1.0851
C2–C3	1.3927	1.4095
C2–C11	1.4383	1.4269
C3–C4	1.3817	1.3963
C3–C10	1.4428	1.4299
C4–C5	1.3853	1.3912
C4–H8	1.0725	1.082
C5–N6	1.3178	1.3366
C5–H9	1.0752	1.0853
C10–N12	1.1288	1.154
C11–N13	1.1292	1.1545
Bond angle (°)		
C2–C1–N6	123.3	123.6
C2–C1–H7	119.6	119.3
N6–C1–H7	117.0	117.0
C1–C2–C3	118.0	117.9
C1–C2–C11	119.5	119.8
C3–C2–C11	122.4	122.1
C2–C3–C4	118.5	118.2
C2–C3–C10	121.6	121.5
C4–C3–C10	119.7	120.1
C3–C4–C5	118.1	118.7
C3–C4–H8	120.8	120.3
C5–C4–H8	120.9	120.9
C4–C5–N6	123.5	123.6
C4–C5–H9	120.0	120.1
N6–C5–H9	116.3	116.2
C1–N6–C5	118.2	117.8
Dihedral angle (°)		
N6–C1–C2–C3	0.0	0.0
N6–C1–C2–C11	180.0	180.0
H7–C1–C2–C3	180.0	180.0
H7–C1–C2–C11	0.0	0.0
C2–C1–N6–C5	0.0	0.0
H7–C1–N6–C5	180.0	180.0
C1–C2–C3–C4	0.0	0.0
C1–C2–C3–C10	180.0	−180.0
C11–C2–C3–C4	180.0	−180.0
C11–C2–C3–C10	0.0	0.0
C2–C3–C4–C5	0.0	0.0
C2–C3–C4–H8	180.0	180.0
C10–C3–C4–C5	−180.0	180.0
C10–C3–C4–H8	0.0	0.0
C3–C4–C5–N6	0.0	0.0
C3–C4–C5–H9	−180.0	−180.0
H8–C4–C5–N6	180.0	180.0
H8–C4–C5–H9	0.0	0.0
C4–C5–N6–C1	0.0	0.0
H9–C5–N6–C1	−180.0	180.0

3. Computational methods

The computations of the geometries, electronic structures, polarizabilities and hyperpolarizabilities, vibrational frequencies as well as electronic absorption spectrum for dye sensitizer 3,4-pyridinedicarbonitrile was done using Hartree–Fock (HF) and density functional theory (DFT) with Gaussian03 package (Frisch et al., 2003). The DFT was treated according to hybrid functional Becke's three parameter gradient-corrected exchange potential and the Lee–Yang–Parr (B3LYP) (Becke, 1993; Miehlich et al., 1989; Lee et al., 1988), and all calculations were performed without any symmetry constraints by using polarized Triple-Zeta 6-311++G(d,p) basis set. The NBO analysis was performed using restricted Hartree–Fock (RHF) with the same basis set. The electronic absorption spectrum requires calculation of the allowed excitations and oscillator strengths. These calculations were done using TD-DFT with PBE1PBE1 functional and same 6-311++G(d,p) basis set in vacuum and solution, and the non-equilibrium version of the polarizable continuum model (PCM) (Barone and Cossi, 1998; Cossi et al., 2003) was adopted for calculating the solvent effects.

4. Results and discussion

4.1. The geometric structure

The optimized geometry of the 3-aminophthalonitrile is shown in Fig. 1, and the selected bond lengths, bond angles and dihedral angles are listed in Table 1. The crystal structure of the exact title compound is not available, the optimized structure can be compared with similar systems for which crystal structures have been solved along with complete optimized bond lengths, bond angles and dihedral angles. The optimized bond lengths of C2–C11 and C3–C10 is 1.4383 and 1.4428 Å, respectively, at B3LYP/6-311++G(d,p) and also well matched with HF/6-311++G(d,p).

4.2. Electronic structures and charges

Natural bond orbital (NBO) analysis was performed in order to analyze the charge populations of the dye 3,4-pyridinedicarbonitrile. Charge distributions in C, N and H atoms were observed because of the different electro-negativity, the electrons transferred from C atoms to C, N atoms, C atoms to H, N atoms to H atom. The natural charges of different groups are the sum of every atomic natural charge in the group. These data indicate that the cyanine and amide groups are acceptors, while the acetic groups are donors, and the charges were transferred through chemical bonds. The frontier molecular orbitals (MO) energies and corresponding density of state of the dye 3,4-pyridinedicarbonitrile is shown in Fig. 2. The HOMO–LUMO gap of the dye 3,4-pyridinedicarbonitrile in vacuum is 5.96 eV.

While the calculated HOMO and LUMO energies of the bare $Ti_{38}O_{76}$ cluster as a model for nanocrystalline are −6.55 and −2.77 eV, respectively, resulting in a HOMO–LUMO gap of 3.78 eV, the lowest transition is reduced to 3.20 eV according to TD-DFT, and this value is slightly smaller than typical band gap of TiO_2 nanoparticles with nm size (Nazeeruddin et al., 2005). Furthermore, the HOMO, LUMO and HOMO–LUMO gap of $(TiO_2)_{60}$ clusters is −7.52, −2.97, and 4.55 eV (B3LYP/VDZ), respectively (Lundqvist et al., 2006). Taking into account of the cluster size effects and the calculated HOMO, LUMO, HOMO–LUMO gap of the dye 3,4-pyridinedicarbonitrile, $Ti_{38}O_{76}$ and $(TiO_2)_{60}$ clusters, we

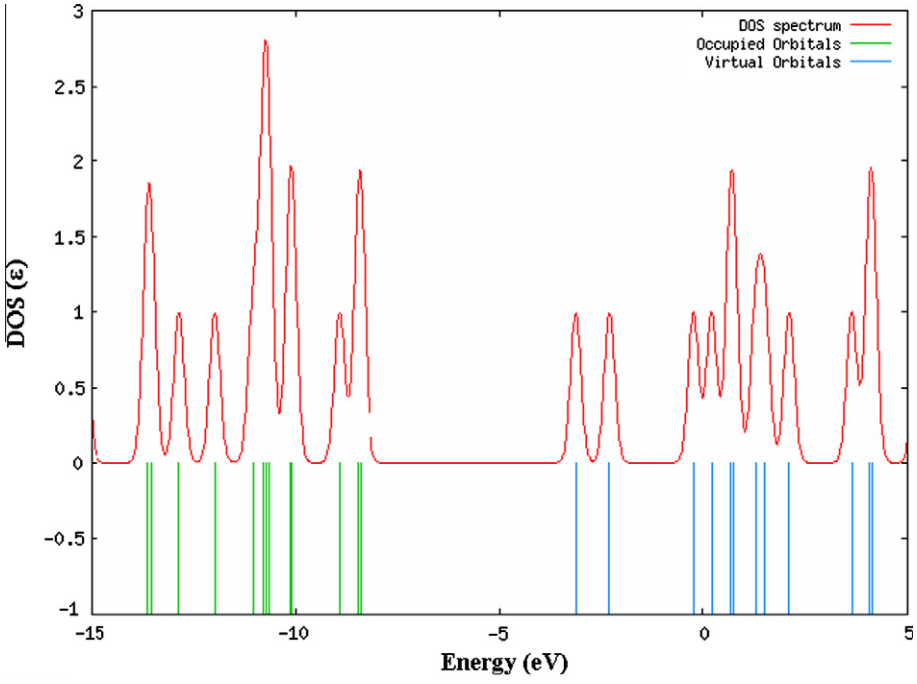

Figure 2 The frontier molecular orbital energies and corresponding density of state (DOS) spectrum of the dye 3,4-pyridinedicarbonitrile by B3LYP/6-311++G(d,p).

can find that the HOMO energies of these dyes fall within the TiO_2 gap.

The above data also reveal the interfacial electron transfer between semiconductor TiO_2 electrode and the dye sensitizer 3,4-pyridinedicarbonitrile is electron injection processes from excited dye to the semiconductor conduction band. This is a kind of typical interfacial electron transfer reaction (Waston and Meyer, 2005).

4.3. IR and Raman frequencies

Figs. 3 and 4 show the observed and calculated IR and Raman spectra of 3,4-pyridinedicarbonitrile, respectively. Pure Lorenzian band shapes were used to estimate the line broadening in the IR and Raman spectra with a band width (FWHM) of 10 cm^{-1}. Comparison of the observed (FT-IR and FT-Raman) and calculated vibrational frequencies of 3,4-pyridinedicarbonitrile is shown in Table 2. Comparison of the frequencies calculated by HF and B3LYP with experimental values reveals the overestimation of the calculated vibrational modes due to neglect of anharmonicity. A corrective vibrational scaling factor of 0.9613 to B3LYP calculated frequencies and scaling factor of 0.8982 to HF calculated frequencies were applied to account for anharmonicity. Inclusion of electron correlation in density functional theory to a certain extent makes the frequency values smaller in comparison with experimental values. Any way notwithstanding the level of calculations it is customary to scale down the calculated harmonic frequencies in order to improve the agreement with the experiment. The strongest IR absorption for 3,4-pyridinedicarbonitrile corresponds to the vibrational mode 28 near about 1614 cm^{-1}, which is corresponding to stretching mode of C═C bonds. The next stronger IR absorption is attributed to vibrational mode 16 near about 867 cm^{-1}, corresponding to the Torsion mode of C–H bonds. In the Raman spectrum, however, the strongest activity mode is the vibrational mode 29 near about 2345 cm^{-1}, which is corresponding to stretching mode of C–N triple bond. The same vibrations computed by HF/6-311 + + G(d,p) and also shows good agreement with experimental data.

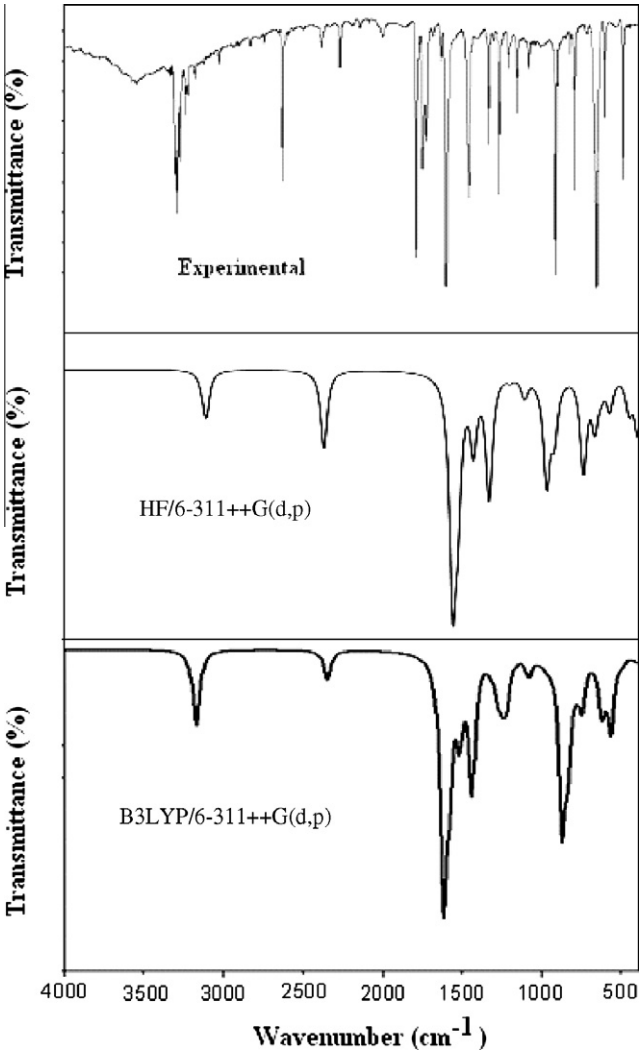

Figure 3 Observed and calculated FT-IR spectra of 3,4-pyridinedicarbonitrile.

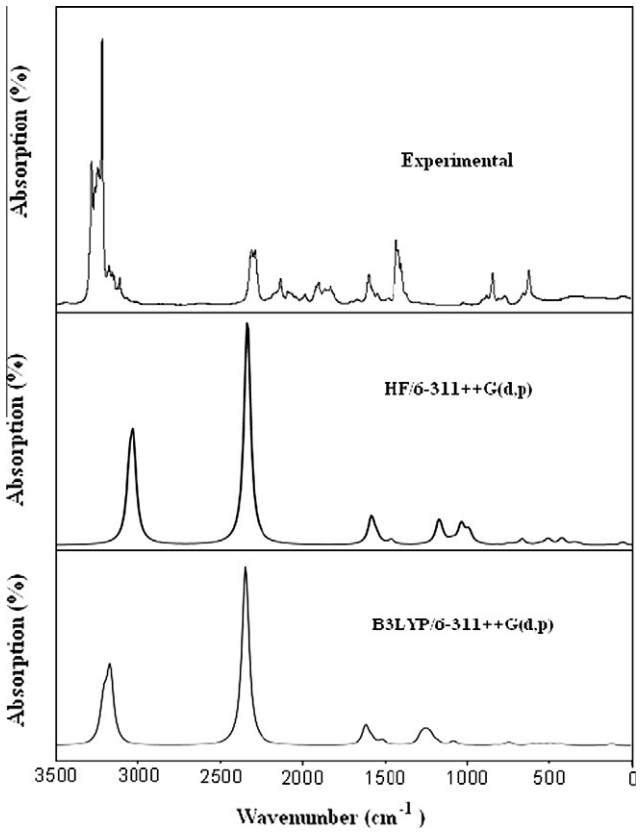

Figure 4 Observed and calculated FT-Raman spectra of 3,4-pyridinedicarbonitrile.

4.4. Polarizability and hyperpolarizability

Polarizabilities and hyperpolarizabilities characterize the response of a system in an applied electric field (Zhang et al., 2004). They determine not only the strength of molecular interactions (long-range intermolecular induction, dispersion forces, etc.) as well as the cross sections of different scattering

and collision processes, but also the nonlinear optical properties (NLO) of the system (Sun et al., 2003; Christiansen et al., 1999). It has been found that the dye sensitizer hemicyanine system, which has high NLO property, usually possesses high photoelectric conversion performance (Wang et al., 2000). In order to investigate the relationships among photocurrent generation, molecular structures and NLO, the polarizabilities and hyperpolarizabilities of 3,4-pyridinedicarbonitrile was calculated.

Here, the polarizability and the first hyperpolarizabilities are computed using B3LYP/6-311 + + G(d,p). The definitions

Table 2 Comparison of the observed (FT-IR and FT-Raman) and calculated vibrational frequencies of 3,4-pyridinedicarbonitrile.

Vibrational mode no	Species	Experimental wavenumber (cm^{-1})		Scaled wavenumber (cm^{-1})		IR intensity	Raman active	Assignments	PED (%)
		FT-IR	FT-Raman	HF/6-311 + + G(d,p)	B3LYP/6-311 + + G(d,p)				
1	A′	–	–	129	114	0.8	1.1	β C–C–N	β C–C–N (98)
2	A′	–	–	129	115	1.5	5.9	β C–C–N	β C–C–N (78)
3	A″	–	–	187	168	9.1	0.04	γ C–C–N	γ C–C–N (69)
4	A′	–	267	218	196	8.0	1.0	δ C–C	δ C–C (91)
5	A″	–	–	412	361	0.5	1.4	δ C–C + γ C–C–N	δ C–C (45) + γ C–C–N (35)
6	A″	–	–	427	384	0.8	0.9	γ C–C	γ C–C (74)
7	A″	–	427	449	420	0.3	4.1	τ C–C–N + γ C–H	τ C–C–N (68) + γ C–H (25)
8	A′	519	–	526	485	0.8	10.0	δ C–C	δ C–C (92)
9	A″	561	–	613	559	11.2	4.9	γ C–C–N + γ C–H	γ C–C–N (70) + γ C–H (21)
10	A″	568	–	624	578	0.5	4.5	γ C–C–N	γ C–C–N (93)
11	A′	643	–	668	616	8.1	1.9	β C–C–C	β C–C–C (97)
12	A′	666	–	682	627	0.3	0.3	β C–C–N + δ C–C	β C–C–N(55) + δ C–C (28)
13	A″	753	–	790	742	7.2	14.3	γ C–H	γ C–H (95)
14	A″	–	819	844	780	1.6	0.4	τ C–C–C + ω C–H	τ C–C–C (81) + ω C–H (11)
15	A′	826	839	884	829	12.1	2.8	β C–H	β C–H (96)
16	A″	869	840	958	867	25.3	0.4	τ C–H	τ C–H (69)
17	A′	848	961	1073	966	1.1	1.3	δ C–C	δ C–C (91)
18	A″	1018	–	1129	1009	0.4	0.3	τ C–H	τ C–H (95)
19	A′	1024	–	1142	1076	3.1	16.6	β C–H	β C–H (88)
20	A′	1180	–	1190	1175	0.2	9.0	δ C–C	δ C–C (76)
21	A′	1214	–	1253	1217	6.4	30.6	υ_{sym} C–C	υ_{sym} C–C (54)
22	A′	1252	–	1322	1245	4.5	31.5	Rb C–C	Rb C–C (73)
23	A′	1293	–	1337	1272	4.3	29.9	υ C–C + υ_{sym} C–C–N	υ C–C (59) + υ_{sym} C–C–N (30)
24	A″	1373	1339	1422	1316	1.3	0.6	γ C–H	γ C–H (93)
25	A′	1466	1451	1554	1435	20.4	0.3	υ C≡N	υ C≡N (98)
26	A′	1544	–	1654	1513	10.6	17.4	υ C–C	υ C–C (92)
27	A′	–	–	1751	1579	13.4	15.9	υ_{asy} C=C	υ_{asy} C=C (74)
28	A′	1661	–	1785	1614	36.1	65.4	υ_{asy} C=C	υ_{asy} C=C (97)
29	A′	2241	2767	2599	2345	4.1	370.5	υ_{asy} C–N	υ_{asy} C–N (91)
30	A′	–	2783	2605	2350	0.6	217.2	υ C≡N	υ C≡N (94)
31	A′	3143	2871	3344	3169	10.5	126.0	υ_{sym} C–H	υ_{sym} C–H (87)
32	A′	3169	2933	3354	3175	1.3	105.9	υ_{sym} C–H	υ_{sym} C–H (93)
33	A′	3422	2961	3378	3211	0.8	125.1	υ C–H	υ C–H (84)

υ – stretching; υ_{sym} – symmetric stretching; υ_{asy} – asymmetric stretching; Rb – ring breathing; β – in plane bending; γ – out-of-plane bending; ω – wagging; τ – torsion; δ – ring deformation.

Table 3 Calculated polarizability (α) of the dye 3,4-pyridinedicarbonitrile (in a.u.) by B3LYP/6-311 + + G(d,p).

α_{xx}	α_{xy}	α_{yy}	α_{xz}	α_{yz}	α_{zz}	α	Δα
129.20	−2.93	107.10	0.00005	−0.00014	47.90	94.73	72.81

Table 4 Calculated hyperpolarizability (β) of the dye 3,4-pyridinedicarbonitrile (in a.u.) by B3LYP/6-311 + + G(d,p).

β_{xxx}	β_{xxy}	β_{xyy}	β_{yyy}	β_{xxz}	β_{xyz}	β_{yyz}	β_{xzz}	β_{yzz}	β_{zzz}	β_{ii}
−37.211	15.721	−6.553	0.112	0.626	−0.009	0.468	0.923	−0.689	0.248	0.806

(Sun et al., 2003; Christiansen et al., 1999) for the isotropic polarizability is

$$\alpha = \frac{1}{3}(\alpha_{XX} + \alpha_{YY} + \alpha_{ZZ}) \quad (1)$$

The polarizability anisotropy invariant is

$$\Delta\alpha = \left[\frac{(\alpha_{XX} - \alpha_{YY})^2 + (\alpha_{YY} - \alpha_{ZZ})^2 + (\alpha_{ZZ} - \alpha_{XX})^2}{2}\right]^{\frac{1}{2}} \quad (2)$$

and the average hyperpolarizability is

$$\beta_{\|} = \frac{1}{5}(\beta_{iiZ} + \beta_{iZi} + \beta_{Zii}) \quad (3)$$

where α_{XX}, α_{YY}, and α_{ZZ} are tensor components of polarizability; β_{iiZ}, β_{iZi}, and β_{Zii} (i from X to Z) are tensor components of hyperpolarizability.

Tables 3 and 4 list the values of the polarizabilities and hyperpolarizabilities of the dye 3,4-pyridinedicarbonitrile. In addition to the individual tensor components of the polarizabilties and the first hyperpolarizabilities, the isotropic polarizability, polarizability anisotropy invariant and hyperpolarizability are also calculated. The calculated isotropic polarizability of 3,4-pyridinedicarbonitrile is 94.73 a.u. However, the calculated isotropic polarizability of JK16, JK17, dye 1, dye 2, D5, DST and DSS is 759.9, 101.5, 694.7, 785.7, 510.6, 611.2 and 802.9 a.u., respectively (Zhang et al., 2009; Seidl et al., 1996). The above data indicate that the donor-con-

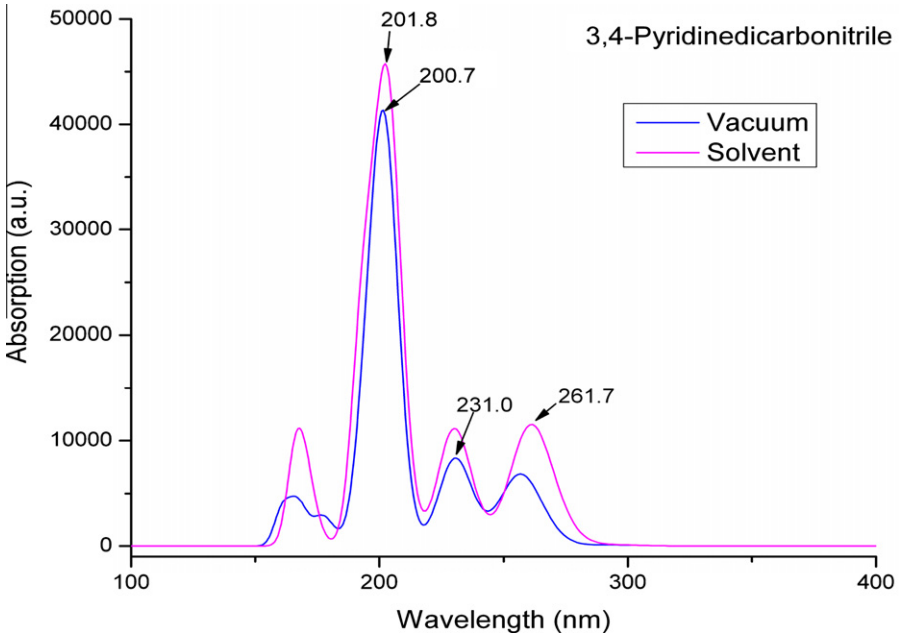

Figure 5 Calculated electronic absorption spectra of the dye 3,4-pyridinedicarbonitrile by TD-PBE1PBE1/6-311 + + G(d,p).

Table 5 Computed excitation energies, electronic transition configurations and oscillator strengths (*f*) for the optical transitions with $f > 0.01$ of the absorption bands in visible and near-UV region for the dye 3,4-pyridinedicarbonitrile in acetonitrile by TD-PBE1PBE1/6-311 + + G(d,p).

State	Configurations composition (corresponding transition orbitals)	Excitation energy (eV/nm)	Oscillator strength (*f*)
2	−0.13 (31 → 34) −0.24 (31 → 35) 0.61 (33 → 34) −0.13 (33 → 35)	4.79/258.55	0.14
4	0.57 (31 → 34) 0.17 (33 → 34) 0.27 (33 → 35)	5.44/227.70	0.14
6	0.12 (27 → 34) −0.26 (31 → 34) 0.54 (33 → 35)	6.17/200.75	0.52
8	−0.13 (28 → 34) 0.60 (31 → 35) 0.12 (33 → 34) −0.12 (33 → 35)	6.47/191.57	0.29
11	−0.11 (27 → 34) 0.63 (28 → 34) 0.10 (29 → 37) 0.12 (31 → 35) −0.12 (32 → 36)	7.24/171.25	0.03
15	0.49 (27 → 34) 0.11 (30 → 36) −0.44 (32 → 36)	7.41/167.31	0.03
18	0.37 (27 → 34) 0.16 (28 → 34) 0.51 (32 → 36)	7.59/163.34	0.06
20	0.10 (27 → 35) 0.67 (32 → 37)	7.97/155.44	0.08

jugate π bridge-acceptor (D-π-A) chain-like dyes have stronger response for external electric field. Whereas, for dye sensitizers D5, DST, DSS, JK16, JK17, dye 1 and dye 2, on the basis of the published photo-to-current conversion efficiencies, the similarity and the difference of geometries, and the calculated isotropic polarizabilities, it is found that the longer the length of the conjugate bridge in similar dyes, the larger the polarizability of the dye molecule, and the lower the photo-to-current conversion efficiency. This may be due to the fact that the longer conjugate-pi-bridge enlarged the delocalization of electrons, thus it enhanced the response of the external field, but the enlarged delocalization may be not favorable to generate charge separated state effectively. So it induces the lower photo-to-current conversion efficiency.

4.5. Electronic absorption spectra and sensitized mechanism

Electronic absorption spectra of 3,4-pyridinedicarbonitrile in vacuum and solvent were performed using TD-DFT(PBE1PBE1)/6-311++G(d,p) calculations, and the results are shown in Fig. 5. It is observed that the absorption in the visible region is much weaker than that in the UV region for 3,4-pyridinedicarbonitrile. The results of TD-DFT have an appreciable red-shift in vacuum and solvent, and the degree of red-shift in solvent is more significant than that in vacuum. The discrepancy between vacuum and solvent effects in TD-DFT calculations may result from two aspects. The first aspect is smaller gap of materials which induces smaller excited energies. The other is solvent effects. Experimental measurements of electronic absorptions are usually performed in solution. Solvent, especially polar solvent, could affect the geometry and electronic structure as well as the properties of molecules through the long-range interaction between solute molecule and solvent molecule. For these reasons it is more difficult to make the TD-DFT calculation is consistent with quantitatively. Though the discrepancy exists, the TD-DFT calculations are capable of describing the spectral features of 3,4-pyridinedicarbonitrile because of the agreement of line shape and relative strength as compared with the vacuum and solvent.

The HOMO–LUMO gap of 3,4-pyridinedicarbonitrile in acetonitrile at PBE1PBE1/6-311++G(d,p) theory level is smaller than that in vacuum. This fact indicates that the solvent effects stabilize the frontier orbitals of 3,4-pyridinedicarbonitrile. So it induces the smaller intensities and red-shift of the absorption as compared with that in vacuum.

In order to obtain the microscopic information about the electronic transitions, the corresponding MO properties are checked. The absorption in visible and near-UV region is the most important region for photo-to-current conversion, so only the 20 lowest singlet/singlet transitions of the absorption band in visible and near-UV region for 3,4-pyridinedicarbonitrile is listed in Table 5. The data of Table 5 and Fig. 6 are based on the 6-311++G(d,p) results with solvent effects involved.

This indicates that the transitions are photoinduced charge transfer processes, thus the excitations generate charge separated states, which should favor the electron injection from the excited dye to semiconductor surface. Commonly, the atom occupied by more densities of HOMO should have stronger ability for detaching electrons, whereas the atom with more

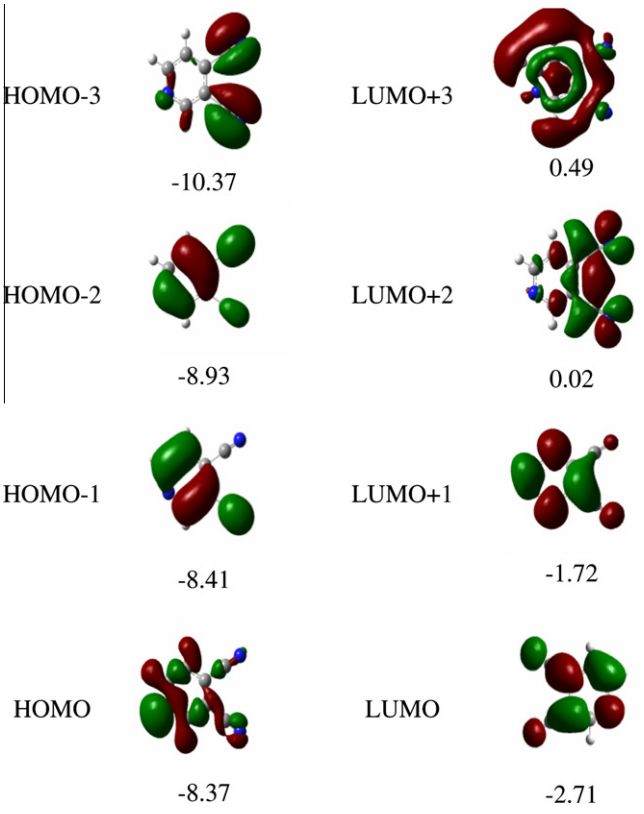

Figure 6 Isodensity plots (isodensity contour = 0.02 a.u.) of the frontier orbitals of the dye 3,4-pyridinedicarbonitrile and corresponding orbital energies (in eV) by TD-PBE1PBE1/6-311++G(d,p).

occupation of LUMO should be easier to gain electrons. For 3,4-pyridinedicarbonitrile, the highest occupied molecular orbital (HOMO) lying at −8.37 eV, is a delocalized π orbital. The HOMO-1, lying −8.41 eV below the HOMO, is a delocalized π orbital over the entire molecule. While the HOMO-2 and HOMO-3, lying −8.93, −10.37 eV below the HOMO, respectively, are π orbitals that localized in benzene ring. Whereas, the lowest unoccupied molecular orbital (LUMO), lying at −2.74 eV, is π* orbital that localized. The LUMO + 1, lying about −1.72 eV above the LUMO, is also a π* orbital that is similar to LUMO. The HOMO–LUMO gap of the dye 3,4-pyridinedicarbonitrile is 5.66 eV.

The solar energy to electricity conversion efficiency (η) under AM 1.5 white-light irradiation can be obtained from the following formula:

$$\eta(\%) = \frac{J_{SC}[\text{mA cm}^{-2}]V_{OC}[V]ff}{I_0[\text{mW cm}^{-2}]} \times 100 \quad (4)$$

where I_0 is the photon flux, J_{sc} is the short-circuit photocurrent density, and V_{oc} is the open-circuit photovoltage, and *ff* represents the fill factor (Zhang et al., 2007). At present, the J_{sc}, the V_{oc}, and the *ff* are only obtained by experiment, the relationship among these quantities and the electronic structure of dye is still unknown. The analytical relationship between V_{oc} and E_{LUMO} may exist. According to the sensitized mechanism (electron injected from the excited dyes to the semiconductor

conduction band) and single electron and single state approximation, there is an energy relationship:

$$eV_{oc} = E_{\mathrm{LUMO}} - E_{CB} \quad (5)$$

where E_{CB} is the energy of the semiconductor's conduction band edge. So the V_{oc} may be obtained applying the following formula:

$$V_{oc} = \frac{(E_{\mathrm{LUMO}} - E_{CB})}{e} \quad (6)$$

It induces that the higher the E_{LUMO}, the larger the V_{oc}. The results of organic dye sensitizer JK16 and JK17 (Zhang et al., 2009a), DST and DSS also proved the tendency (Zhou et al., 2008) (JK16: $E_{\mathrm{LUMO}} = -2.73$ eV, $V_{oc} = 0.74$ V; JK17: $E_{\mathrm{LUMO}} = -2.87$ eV, $V_{oc} = 0.67$ V; DSS: $E_{\mathrm{LUMO}} = -2.91$ eV, $V_{oc} = 0.70$ V; D-ST: $E_{\mathrm{LUMO}} = -2.83$ eV, $V_{oc} = 0.73$ V). Certainly, this formula expects further test by experiment and theoretical calculation**.** The J_{sc} is determined by two processes, one is the rate of electron injection from the excited dyes to the conduction band of semiconductor, and the other is the rate of redox between the excited dyes and electrolyte. Electrolyte effect on the redox processes is very complex, and it is not taken into account in the present calculations. This indicates that most of excited states of 3,4-pyridinedicarbonitrile have larger absorption coefficient, and then with shorter lifetime for the excited states, so it results in the higher electron injection rate which leads to the larger J_{sc} of 3,4-pyridinedicarbonitrile. On the basis of above analysis, it is clear that the 3,4-pyridinedicarbonitrile has better performance in DSSC.

5. Conclusions

The geometries, electronic structures, polarizabilities, and hyperpolarizabilities of dye 3,4-pyridinedicarbonitrile was studied by using ab initio HF and DFT with hybrid functional B3LYP, and the UV–Vis spectra were investigated by using TD-DFT methods. The NBO results suggest that 3,4-pyridinedicarbonitrile is a (D-π-A) system. The calculated isotropic polarizability of 3,4-pyridinedicarbonitrile is 94.73 a.u. The calculated polarizability anisotropy invariant of 3,4-pyridinedicarbonitrile is 72.81 a.u. The hyperpolarizability of 3,4-pyridinedicarbonitrile is 0.80 (in a.u). The frequency of strongest IR absorption for 3,4-pyridinedicarbonitrile is 1614 cm^{-1} and the frequency of strongest Raman activity for 3,4-pyridinedicarbonitrile is 2345 cm^{-1}. The electronic absorption spectral features in visible and near-UV region were assigned based on the qualitative agreement to TD-DFT calculations. The absorptions are all ascribed to $\pi \rightarrow \pi^*$ transition. The three excited states with the lowest excited energies of 3,4-pyridinedicarbonitrile is photoinduced electron transfer processes that contributes sensitization of photo-to-current conversion processes. The interfacial electron transfer between semiconductor TiO_2 electrode and dye sensitizer 3,4-pyridinedicarbonitrile is electron injection process from excited dye as donor to the semiconductor conduction band. Based on the analysis of geometries, electronic structures, and spectrum properties of 3,4-pyridinedicarbonitrile, the role of cyanine in phthalonitrile is as follows: it enlarged the distance between electron donor group and semiconductor surface, and decreased the timescale of the electron injection rate, resulted in giving lower conversion efficiency. This indicates that the choice of the appropriate conjugate bridge in dye sensitizer is very important to improve the performance of DSSC.

Acknowledgements

This work was partly financially supported by University Grants Commission, Govt. of India, New Delhi, within the Major Research Project scheme under the approval-cum-sanction No. F.No.34-5/2008 (SR) and 34-1/TN/08.

References

Barone, V., Cossi, M., 1998. J. Phys. Chem. A 102, 1995.
Becke, A.D., 1993. J. Chem. Phys. 98, 5648.
Campbell, W.M., Burrell, A.K., Officer, D.L., Jolley, K.W., 2004. Coord. Chem. Rev. 248, 1363.
Chiba, Y., Islam, A., Watanabe, Y., Komiya, R., Koide, N., Han, L., 2006. Jpn. J. Appl. Phys. 45, L638.
Christiansen, O., Gauss, J., Stanton, J.F., 1999. Chem. Phys. Lett. 305, 147.
Cossi, M., Rega, N., Scalmani, G., Barone, V., 2003. J. Comput. Chem. 24, 669.
Edvinsson, T., Li, C., Pschirer, N., Schoneboom, J., Eickemeyer, F., Sens, R., Boschloo, G., Herrmann, A., Mullen, K., Hagfeldt, A., 2007. J. Phys. Chem. C 111, 15137.
Frisch, M.J., Trucks, G.W., Schlegel, H.B., Scuseria, G.E., Robb, M.A., Cheeseman, J.R., Montgomery Jr., J.A., Vreven, T., Kudin, K.N., Burant, J.C., Millam, J.M., Iyengar, S.S., Tomasi, J., Barone, V., Mennucci, B., Cossi, M., Scalmani, G., Rega, N., Petersson, G.A., Nakatsuji, H., Hada, M., Ehara, M., Toyota, K., Fukuda, R., Hasegawa, J., Ishida, M., Nakajima, T., Honda, Y., Kitao, O., Nakai, H., Klene, M., Li, X., Knox, J.E., Hratchian, H.P., Cross, J.B., Adamo, C., Jaramillo, J., Gomperts, R., Stratmann, R.E., Yazyev, O., Austin, A.J., Cammi, R., Pomelli, C., Ochterski, J.W., Ayala, P.Y., Morokuma, K., Voth, G.A., Salvador, P., Dannenberg, J.J., Zakrzewski, V.G., Dapprich, S., Daniels, A.D., Strain, M.C., Farkas, O., Malick, D.K., Rabuck, A.D., Raghavachari, K., Foresman, J.B., Ortiz, J.V., Cui, Q., Baboul, A.G., Clifford, S., Cioslowski, J., Stefanov, B.B., Liu, G., Liashenko, A., Piskorz, P., Komaromi, I., Martin, R.L., Fox, D.J., Keith, T., Al-Laham, M.A., Peng, C.Y., Nanayakkara, A., Challacombe, M., Gill, P.M.W., Johnson, B., Chen, W., Wong, M.W., Gonzalez, C., Pople, J.A., 2003. Gaussian 03. Gaussian Inc., Pittsburgh, PA.
Gratzel, M., 2001. Nature 414, 338.
Hagberg, D.P., Edvinsson, T., Marinado, T., Boschloo, G., Hagfeldt, A., Sun, L., 2006. Chem. Commun., 2245.
Hara, K., Kurashige, M., Dan-oh, Y., Kasada, C., Shinpo, A., Suga, S., Sayama, K., Arakawa, H., 2003a. New J. Chem. 27, 783.
Hara, K., Sato, T., Katoh, R., Furube, A., Ohga, Y., Shinpo, A., Suga, S., Sayama, K., Sugihara, H., Arakawa, H., 2003b. J. Phys. Chem. B 107, 597.
Horiuchi, T., Miura, H., Sumioka, K., Uchida, S., 2004. J. Am. Chem. Soc. 126, 12218.
Ito, S., Miura, H., Uchida, S., Takata, M., Sumioka, K., Liska, P., Comte, P., Pechy, P., Gratzel, M., 2008. Chem. Commun., 5194.
Kim, S., Lee, J.W., Kang, S.O., Ko, J., Yum, J.H., Fantacci, S., De Angellis, F., Di Censo, D., Nazeeruddin, M.K., Gratzel, M., 2006. J. Am. Chem. Soc. 128, 16701.
Kitamura, T., Ikeda, M., Shigaki, K., Inoue, T., Anderson, N.A., Ai, X., Lian, T., Yanagida, S., 2004. Chem. Mater. 16, 1806.

Koumura, N., Wang, Z.S., Mori, S., Miyashita, M., Suzuki, E., Hara, K., 2006. J. Am. Chem. Soc. 128, 14256.
Lee, C., Yang, W., Parr, R.G., 1988. Phys. Rev. B 37, 785.
Li, S.L., Jiang, K.J., Shao, K.F., Yang, L.M., 2006. Chem. Commun., 2792.
Liang, M., Xu, W., Cai, F., Chen, P., Peng, B., Chen, J., Li, Z., 2007. J. Phys. Chem. C 111, 44652.
Lin, J.T., Chen, P.C., Yen, Y.S., Hsu, Y.C., Chou, H.H., Yeh, M.C.P., 2009. Org. Lett. 11, 97.
Lundqvist, M.J., Nilsing, M., Persson, P., Lunell, S., 2006. Int. J. Quantum Chem. 106, 3214.
Miehlich, B., Savin, A., Stoll, H., Preuss, H., 1989. Chem. Phys. Lett. 157, 200.
Nazeeruddin, M.K., De Angelis, F., Fantacci, S., Selloni, A., Viscardi, G., Liska, P., Ito, S., Takeru, B., Gratzel, M., 2005. J. Am. Chem. Soc. 127, 16835.
Park, N.G., Kim, K., 2008. Phys. Status Solidi a 205, 1895.
Regan, B.O., Gratzel, M., 1991. Nature 353, 737.
Seidl, A., Gorling, A., Vogl, P., Majewski, J.A., Levy, M., 1996. Phys. Rev. B 53, 3764.
Shi, D., Pootrakuchote, N., Yi, Z., Xu, M., Zakeeruddin, S.M., Gratzel, M., Wang, P., 2008. J. Phys. Chem. C 112, 17478.
Sun, Y., Chen, X., Sun, L., Guo, X., Lu, W., 2003. Chem. Phys. Lett. 381, 397.
Thomas, K.R.J., Lin, J.T., Hsu, Y.C., Ho, K.C., 2005. Chem. Commun. 1, 4098.
Wang, Z.S., Huang, Y.Y., Huang, C.H., Zheng, J., Cheng, H.M., Tian, S.J., 2000. Synth. Met. 14, 201.
Wang, Z.S., Cui, Y., Hara, K., Dan-oh, Y., Kasada, C., Shinpo, A., 2007. Adv. Mater. 19, 1138.
Wang, M., Xu, M., Shi, D., Li, R., Gao, F., Zhang, G., Yi, Z., Humphry-Baker, R., Wang, P., Zakeeruddin, S.M., Gratzel, M., 2008. Adv. Mater. 20, 4460.
Waston, D.F., Meyer, G.J., 2005. Annu. Rev. Phys. Chem. 56, 119.
Xu, W., Peng, B., Chen, J., Liang, M., Cai, F., 2008. J. Phys. Chem. C 112, 874.
Xu, M., Wenger, S., Bara, H., Shi, D., Li, R., Zhou, Y., Zakeeruddin, S.M., Gratzel, M., Wang, P., 2009. J. Phys. Chem. C 113, 2966.
Zhang, C.R., Chen, H.S., Wang, G.H., 2004. Chem. Res. Chin. U 20, 640.
Zhang, X.H., Li, C., Wang, W.B., Cheng, X.X., Wang, X.S., Zhang, B.W., 2007. J. Mater. Chem. 17, 642.
Zhang, C.R., Liu, Z.J., Chen, Y.H., Chen, H.S., Wu, Y.Z., Yuan, L.H., 2009a. J. Mol. Struct. 899, 86.
Zhang, C.R., Wu, Y.Z., Chen, Y.H., Chen, H.S., 2009b. Acta Phys. Chim. Sin. 25, 53.
Zhang, G., Bai, Y., Li, R., Shi, D., Wenger, S., Zakeeruddin, S.M., Gratzel, M., Wang, P., 2009c. Energy Environ. Sci. 2, 92.
Zhou, G., Pschirer, N., Schoneboom, J.C., Eickemeyer, F., Baumgarten, M., Mullen, K., 2008. Chem. Mater. 20, 1808.